J Oceanogr (2011) 67:127–133
DOI 10.1007/s10872-011-0002-y

SHORT CONTRIBUTION

ENSO-induced interannual variability in the southeastern South China Sea

Qinyan Liu · Ming Feng · Dongxiao Wang

Received: 25 June 2010 / Revised: 28 September 2010 / Accepted: 29 October 2010 / Published online: 16 February 2011

Abstract In this study, El Niño Southern Oscillation (ENSO)-induced interannual variability in the South China Sea (SCS) is documented using outputs from an eddy-resolving data-assimilating model. It is suggested that during an El Niño (La Niña) event, off-equatorial upwelling (downwelling) Rossby waves induced by Pacific equatorial wind anomalies impinge on the Philippine Islands and excite upwelling (downwelling) coastal Kelvin waves that propagate northward along the west coast of the Philippines after entering the SCS through the Mindoro Strait. The coastal Kelvin waves may then induce negative (positive) sea level anomalies in the southeastern SCS and larger (smaller) volume transport through the Mindoro and Luzon Straits during an El Niño (La Niña) event.

Keywords ENSO · Coastal Kelvin waves · Mindoro Strait · Luzon Strait · Bluelink model

1 Introduction

The South China Sea (SCS) is a semi-enclosed marginal sea in the western Pacific, connecting the Pacific Ocean through the Luzon and Taiwan Straits to the east and the Indonesian Seas and Sulu Sea through the Karimata and Mindoro Straits to the south (Fig. 1). Sea surface temperature (SST) variability and heat balance in the SCS are important to its regional climate. Air–sea heat fluxes in the SCS are influenced by El Niño Southern Oscillation (ENSO) events through atmospheric teleconnection (Klein et al. 1999; Wang et al. 2006a). Oceanic exchange between the SCS and the Pacific through the Luzon Strait is also modulated by ENSO (Qu et al. 2004), though ENSO influences from the low-latitude channels on the SCS have not been documented.

ENSO-related sea level (thermocline) anomalies in the tropical Pacific propagate westward as equatorial and off-equatorial Rossby waves. After impinging on the western boundary of the Pacific, part of the Rossby wave energy is reflected as equatorial Kelvin waves, while part of the energy is able to penetrate through narrow gaps at the western boundary and into the eastern Indian Ocean along the northwest coast of Australia as coastal Kelvin waves (Clarke and Liu 1994; Feng et al. 2003, 2004; Spall and Pedlosky 2005).

In this study, outputs from an eddy-resolving data-assimilating hydrodynamic model are used to document that the ENSO-related sea level (thermocline) signals at the equatorial western Pacific can also penetrate into the southeastern SCS, through the narrow Mindoro Strait, and propagate northward as coastal Kelvin waves along the west coast of the Philippines to reach the northern tip of the Luzon Island (Fig. 1). The ENSO-related variability in the volume transports through the Mindoro and Luzon Straits is also documented.

2 Data and model output

The hydrodynamic model output used in this study was derived from the Bluelink ReANalysis (BRAN), which was

Q. Liu · D. Wang
Key Laboratory of Tropical Marine Environmental Dynamics, South China Sea Institute of Oceanology, Chinese Academy of Sciences, Guangzhou 510301, People's Republic of China

M. Feng (✉)
CSIRO Marine and Atmospheric Research, Underwood Avenue, Floreat, WA 6014, Australia
e-mail: ming.feng@csiro.au

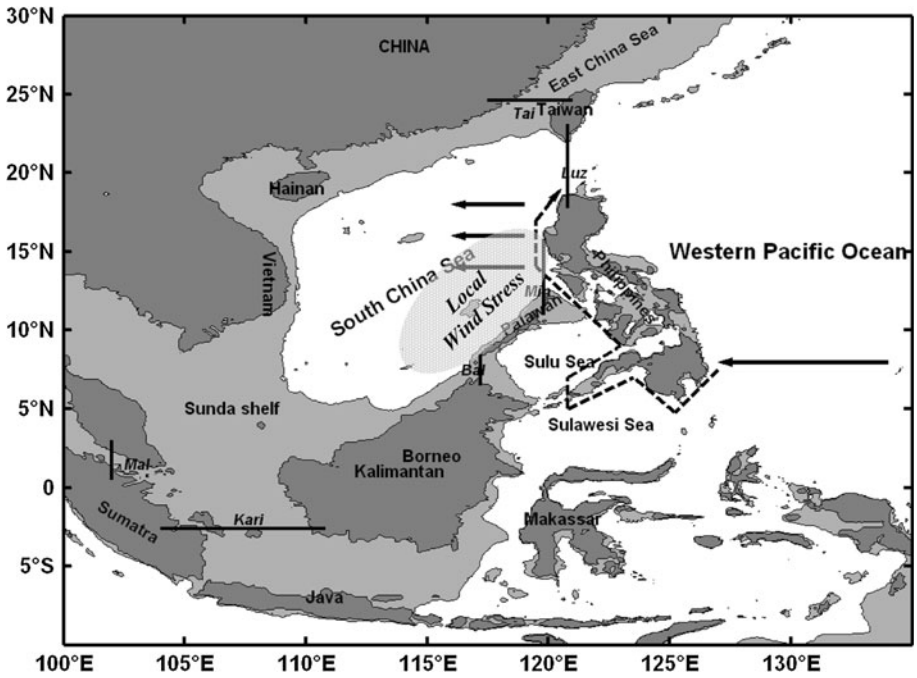

Fig. 1 Geography of the South China Sea and its surrounding region. *Lightly shaded areas* denote water depth shallower than 200 m as derived from the ETOPO5 dataset. A schematic of the planetary wave propagation from the Pacific into the southeastern SCS is shown with *solid* and *dashed arrows*. The *bold lines* are chosen for estimating the respective volume transports through Luzon, Taiwan, Karimata, Mindoro, Balabac, and Malacca Straits from BRAN

based on a global ocean model called OFAM (Ocean Forecasting Australia Model). OFAM was developed as part of the Bluelink partnership between the Commonwealth Scientific and Industrial Research Organisation (CSIRO), the Bureau of Meteorology (BoM), and the Royal Australian Navy (Schiller et al. 2008). BRAN was forced by the European Centre for Medium-Range Weather Forecasts (ECMWF) wind stress, heat and freshwater fluxes; it also assimilated satellite (including altimeter) and in situ data. The model has 0.1° horizontal resolution inside the Australia region (90°E–180°, south of 16.5°N). Outside of this domain, the horizontal resolution decreases to 0.9° across the Pacific and Indian basins and to 2° in the Atlantic Ocean. In the SCS, the zonal resolution is 0.1°, and the meridional resolution is variable with latitude (the resolution south of 16.5°N is 0.1°, and decreases to 0.8° near 24.6°N). In the vertical, BRAN has 47 levels with 10-m resolution from the surface down to 200-m depth. BRAN was used to generate the 1993–2008 archives of daily ocean currents, sea surface height, salinity, and temperature in three dimensions. The BRAN model resolves the Mindoro Strait well: at the southern Panay Sill, it has a sill depth of about 500 m and a channel width of about 50 km at 200-m depth (Fig. 2). The model captures the bottom-trapped outflow from the SCS, though the extent of the outflow reaches a shallower depth compared to observations (Tessler et al. 2010).

The merged (T/P or Jason-1 plus ERS-1/2 or Envisat) weekly sea level data (http://www.jason.oceanobs.com) is used. It covers the globe with 1/3° resolution on a Mercator grid from October 1992. The European Remote Sensing (ERS) monthly wind stress data is obtained from the CERSAT (Centre ERS d'Archivage et de Traitement, *French ERS Processing and Archiving Facility*), at IFREMER (French Research Institute for Exploitation of the Sea), Plouzané (France) (http://www.ifremer.fr/cersat/en/data/). The wind stress data covers the globe from 79.5°S to 79.5°N with 1° horizontal resolution, spanning from March 1992 to December 2000. The Niño 3.4 index is obtained from the Climate Prediction Center of the National Oceanic and Atmospheric Administration. Gridded temperature anomaly fields from monthly mean climatologies, after correcting for instrumental biases of bathythermograph data and after correcting or excluding some Argo float data (Levitus et al. 2005), are obtained from National Oceanographic Data Center.

3 BRAN simulation of seasonal ocean circulation of the SCS

Although BRAN does not resolve the northern SCS with high horizontal resolution, the seasonal ocean circulation in the SCS under the monsoonal wind forcing is reasonably reproduced by BRAN (Fig. 3): a double-gyre during boreal summer, with an anti-cyclonic (cyclonic) circulation in the south (north) (Fig. 3, top); a strong southward western boundary current driven by northeast monsoonal wind during boreal winter (Fig. 3, bottom). These circulation patterns are consistent with a recent review by Hu et al. (2000).

The average westward volume transport across the Luzon Strait is 4.81 Sv in BRAN. The average outflow

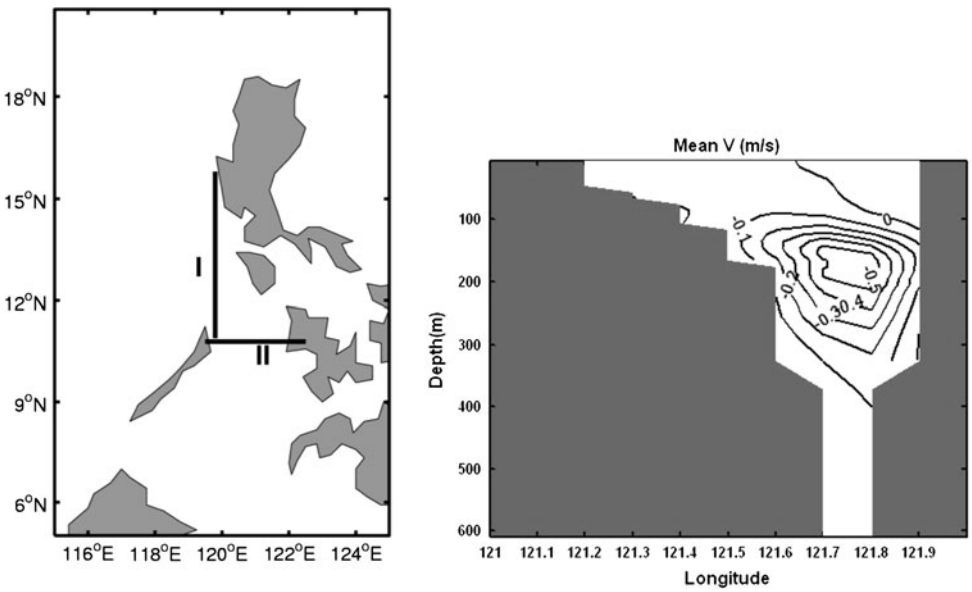

Fig. 2 *Left panel* two sections chosen to estimate the volume transport through the Mindoro Strait. *Right panel* the average meridional velocity across the southern section (section *II*) near the Panay Sill (11°N). The volume transports across the two sections are almost identical in BRAN

volume transports across the Taiwan, Karimata, and Mindoro Straits are 1.44, 1.42, and 2.27 Sv respectively, which are within the range of early estimates, except for the Mindoro Strait (Table 1; Metzger and Hurlburt 1996; Qu 2000; Su 2004; Tian et al. 2006; Cai et al. 2005; Dong et al. 2008; Fang et al. 2009). Using satellite-derived sea surface height and ocean bottom pressure measurements and rectangular hydraulic control theory and geostrophic control, Qu and Song (2009) estimate a full-water column transport of 2.4 Sv and a bottom layer transport of 1.3 Sv. Summing up volume transport through all channels of the SCS, including the minor volume transports through the Balabac and Malacca Straits (Table 1), there is a 0.58-Sv imbalance in the BRAN transport. This is owing to the data-assimilating nature of BRAN, which may not conserve volume properly.

The transport through the Luzon Strait is westward over the annual cycle, with a peak occurring in December (Fig. 4, top panel). The outflow through the Karimata Strait has a maximum southward transport during boreal winter and is northward during summer. The annual transport through the Taiwan Strait is mostly northward, being strong in summer and weak in winter, and the maximum outflow through the Mindoro Strait occurs during October to November. The seasonality of the volume transports through these four Straits in BRAN is similar to results derived from an inverse model (Yaremchuk et al. 2009; Fig. 4, lower panel).

4 ENSO-related interannual variations in the SCS

In BRAN, as well as in the altimeter data (not shown), sea level anomalies (SLA) off the Philippines in the western Pacific are negatively correlated with Niño 3.4 SST at a 4-month lead time, as Rossby wave responses in the western Pacific generated by equatorial wind anomalies (Fig. 5). The negative correlation increases to about −0.7 at the zero-month lead time and has penetrated into the southeastern SCS from the southern tip of the Philippine Islands. It is likely that part of the Pacific Rossby wave energy has been converted into coastal Kelvin wave energy that propagates around the Philippine Islands. The width of the Mindoro Strait is about half of the mean baroclinic Rossby deformation radius at this latitude (∼100 km); thus, the transmission of coastal Kelvin waves can be quite efficient (100%) as derived from a theoretical rotating-hydraulics model (Johnson and Garrett 2006). The Kelvin wave signals can be tracked northward along waveguide off the west coast of the Philippine Islands, reaching the Luzon Strait. Rossby waves may have radiated from the coastal Kelvin waves and propagated into the interior SCS.

Coastal tide gauge sea level records show that it takes less than 2 weeks for the low frequency signals to propagate from Davao to Manila (not shown). Thus, a Hovmoeller diagram of sea level anomalies cannot capture the alongshore propagation of the interannual coastal Kelvin wave accurately. However, historical temperature data have significant, coastally trapped correlations with the Niño 3.4 index in the upper ocean off the west coast of the Philippines, with a peak correlation above −0.4 at the thermocline depth (Fig. 6). The correlations between BRAN temperature anomalies and the Niño 3.4 index have a similar structure, and with a peak correlation above −0.6. These would be indirect evidence of the existence of coastal Kelvin waves along the Philippines coast.

At 4-month lag time, the negative correlations in the southeastern SCS off the west coast of the Philippine

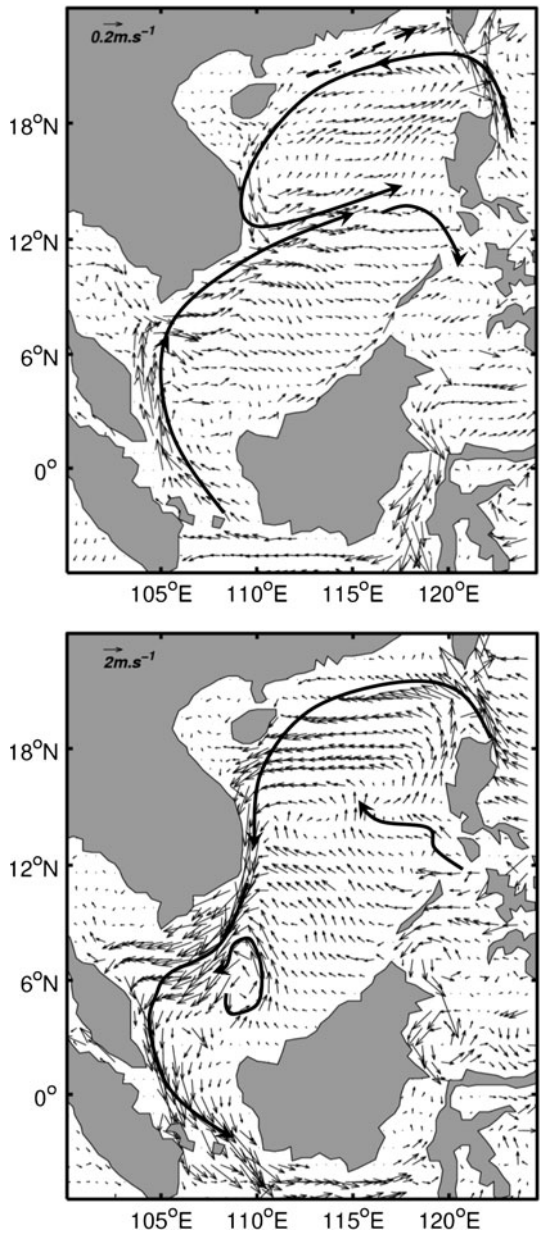

Fig. 3 Average boreal summer (*top*) and winter (*bottom*) surface currents in the SCS from BRAN

Table 1 Average volume transports estimated for various channels of the SCS

	Volume transports (Sv)					
	Luzon	Taiwan	Karimata	Mindoro	Balabac	Malacca
Cai et al. (2005)	−4.06	2.01	2.26	−0.12	−0.08	–
Dong et al. (2008)	−4.64	0.43	3.74	0.45	0.11	–
Fang et al. (2009)	−4.80	1.71	1.16	1.35	0.41	0.16
This study	−4.81	1.44	1.42	2.27	−0.01	0.27

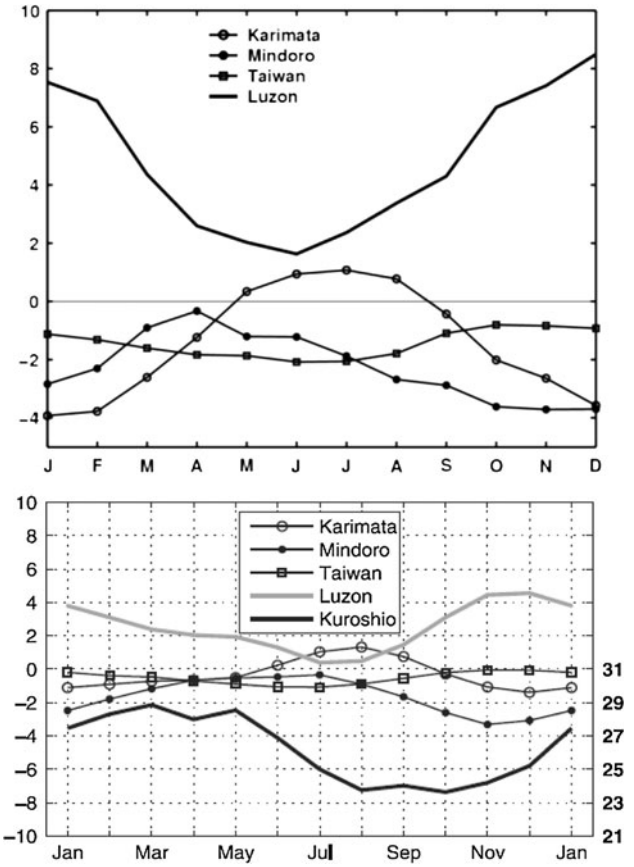

Fig. 4 Monthly climatology of volume transports (Sv) through different straits of the SCS. BRAN (*top*) and an inverse model (*bottom*, from Yaremchuk et al. 2009, Fig. 6 top). Positive transport denotes transport into the SCS

Islands increase to about −0.7, whereas the correlations in the western Pacific start to decay (Fig. 5). The correlation pattern between the SLA and Niño 3.4 index at its peak is similar to the first Empirical Orthogonal Function (EOF) mode of SLA in the SCS (Fang et al. 2006); thus, the ENSO-related SLA variation in the southeastern SCS is the dominant mode of sea level variability in the SCS. The correlation between the SLA in the SCS and Niño 3.4 index becomes less significant at 8-month lag time (Fig. 5).

Interannual anomalies of the outflow through the Mindoro Strait have similar magnitude and are almost out of phase with those through the Luzon Strait (maximum correlation of −0.83 at zero-lag) (Fig. 7). During the peak of the 1997/98 El Niño event, there was an almost 4-Sv increase in volume transport through the Luzon Strait into the SCS, while the outflow from the Mindoro Strait also increased by more than 2 Sv; the opposite occurred during the 1999 and 2000 La Niña event. The correlations between the two transport time series and the Niño 3.4 index are both about 0.7, with the Niño 3.4 index lagging for 2 months. The Karimata Strait transport is not significantly correlated with the Niño 3.4 index. The high

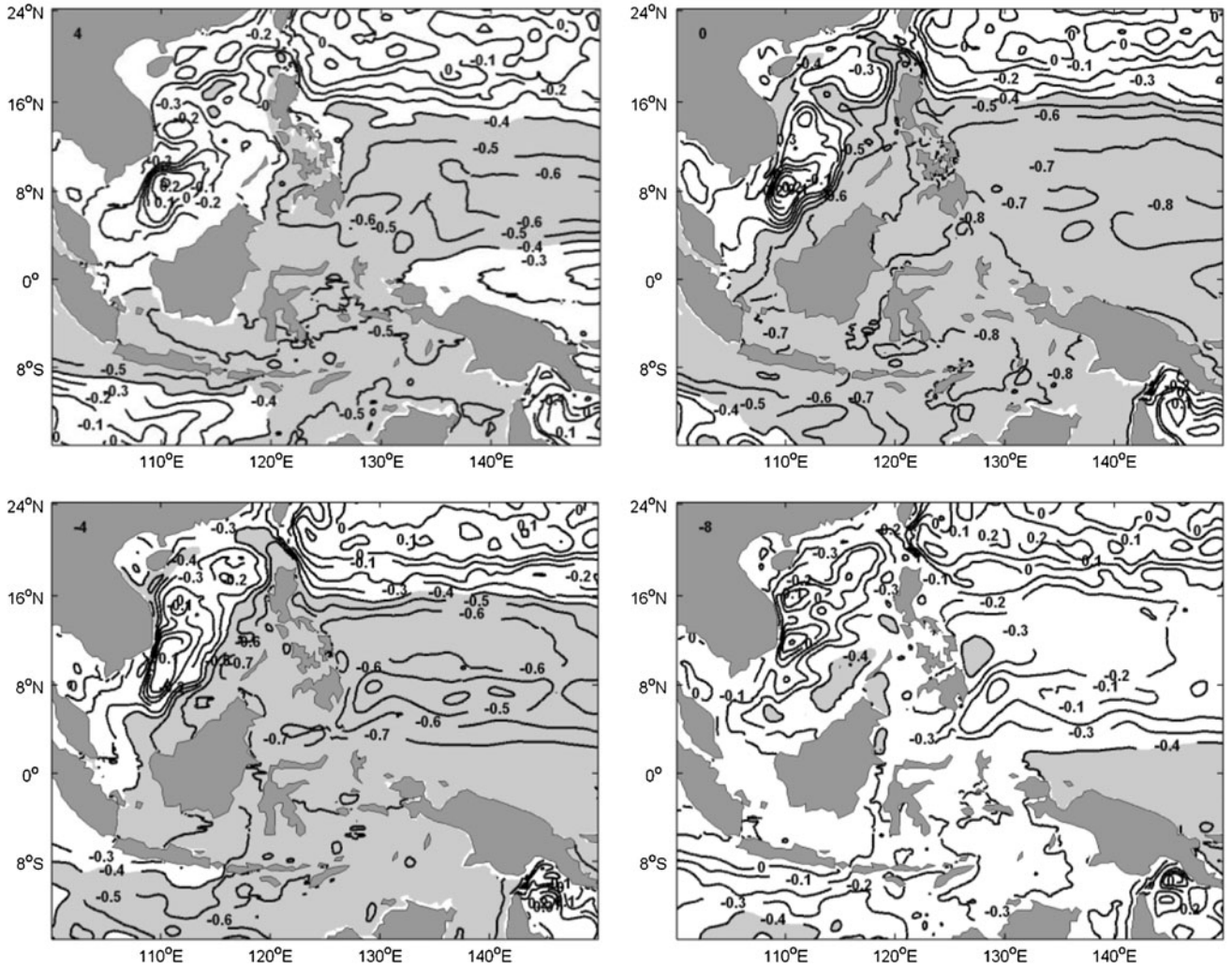

Fig. 5 Correlation coefficients between BRAN's sea surface height anomalies and the Niño 3.4 index at a lead time (in months) of 4 (*top left*), 0 (*top right*), −4 (*bottom left*), −8 (*bottom right*). Values less than −0.4, which have passed 95% significance for 24 degrees of freedom, are *shaded*. Contour interval is 0.1

correlations between the transport anomalies through the Luzon and Mindoro straits are consistent with the coastal Kelvin wave propagation, and the ENSO-related transport anomalies through the Luzon Strait are likely partly driven by coastal Kelvin waves. The results are consistent with Wang et al. (2006b), i.e., remote wind forcing influences the SCS throughflow transports through planetary wave propagations.

Wind stress curl anomaly in the southeastern SCS is highly correlated with the Niño 3.4 indices (−0.61). The correlation between the SLA and the zonal wind stress curl anomalies in the southeastern SCS is 0.44, slightly higher than the correlation between the SLA and the meridional wind stress anomalies, −0.36 (not shown). Thus, local winds may play a lesser role in generating the ENSO-related SLA anomalies in the southeastern SCS, compared with remote forced signals. Numerical model simulation

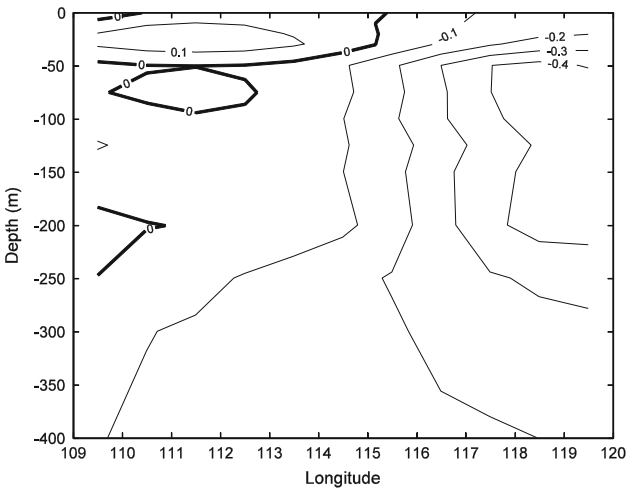

Fig. 6 Linear correlations between annual mean temperature anomaly observations along 15.5°N during 1955–2003 and the Niño 3.4 index

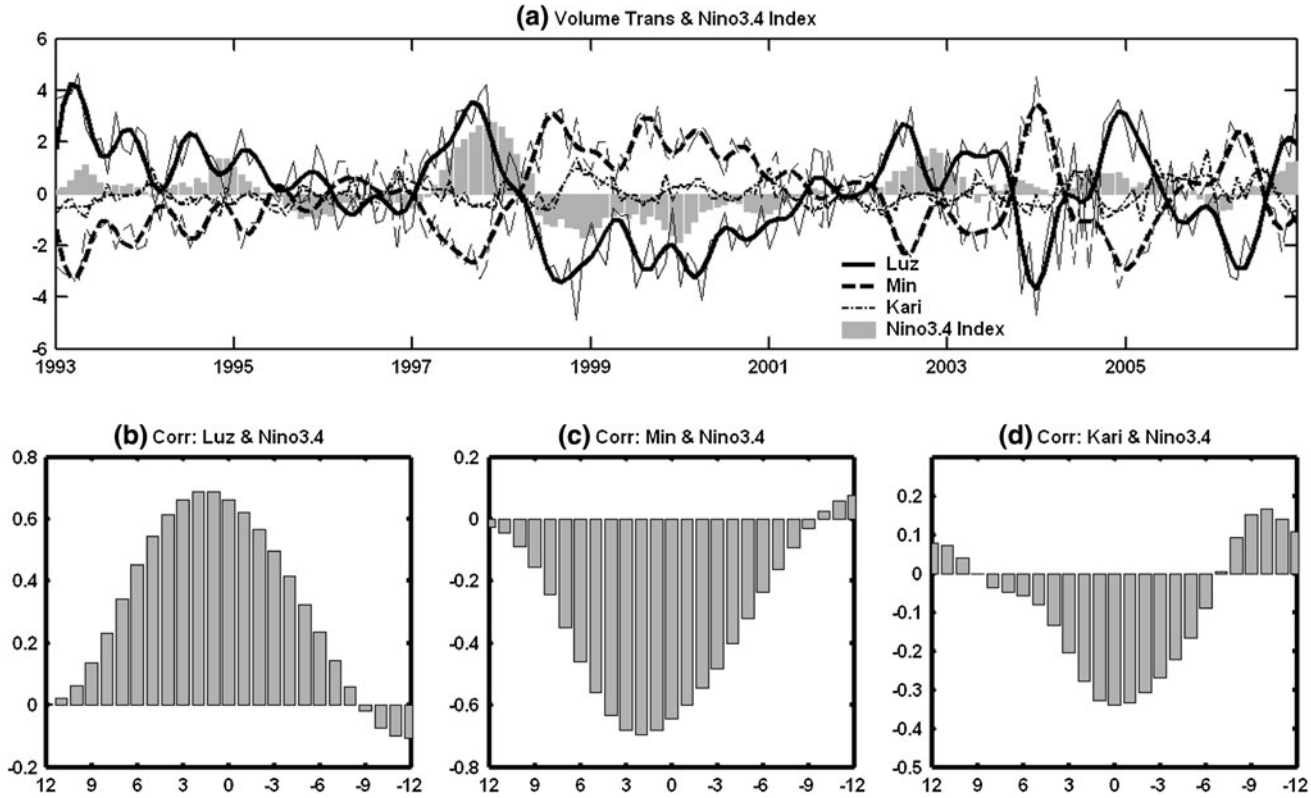

Fig. 7 **a** Interannual anomalies of the volume transports through the Luzon, Mindoro, Karimata Straits, integrated from surface to ocean bottom along the bold line in Fig. 2 (*bold/solid lines* are smoothed time series and positive values denote transport going into the SCS), and the Niño 3.4 index (*shaded*). **b–d** Lag correlations of volume transport anomalies through Luzon, Mindoro, and Karimata Straits with the Niño 3.4 index (horizontal axis denotes time lag in months). Assume the sample number $n = 24$, the critical value $t_\alpha = 2.074$ with 95% significance level. Then the critical value of the coefficient $r_c = \sqrt{\frac{t_\alpha^2}{n-2+t_\alpha^2}} = 0.4044$

has confirmed the transmission of Pacific Rossby wave signals through the Mindoro Strait into the SCS, generated by wind anomalies over the equatorial Pacific (about 5% of total Pacific Rossby wave energy, based on a replication of a model experiment designed by Spall and Pedlosky 2005, not shown).

5 Summary

Using data-assimilating numerical model output and historical datasets, this study has documented the ENSO-related interannual variability of sea level (thermocline) and ocean circulation in the southeastern SCS. It is hypothesized that ENSO-related off-equatorial Rossby waves in the western Pacific may have penetrated into the southeastern SCS through the Mindoro Strait and propagated along the west coast of the Philippine Islands northward as coastal Kelvin waves. The interannual coastal Kelvin waves may have induced the ENSO-related volume transport anomalies across the Mindoro and Luzon Straits. These processes affect regional ocean circulation in the southeastern SCS similar to those with which the ENSO signals affect the ocean circulation in the southeastern Indian Ocean. Although a coarse-resolution ocean model simulation has supported this hypothesis, high spatial resolution modeling with realistic bathymetry is necessary to corroborate results from this study.

Acknowledgments This research was funded by the Knowledge Innovation Program of the Chinese Academy of Sciences (Grant No. kZCX2-YW-214, KZCX2-YW-Q11-02) and the National Natural Science Foundation of China (Grant No. 40806005, 40520140074). This work was also partially supported by a grant from the South China Sea Institute of Oceanology, Chinese Academy of Sciences (Project number SQ200814). This research is partly supported by CSIRO Wealth from Ocean Flagship, CSIRO Julius Award, and Western Australia Marine Science Institute. We would like to thank two anonymous reviewers for constructive comments.

References

Cai SQ, Liu HL, Li W, Long XM (2005) Application of LICOM to the numerical study of the water exchange between the South China Sea and its adjacent oceans. Acta Oceanol Sin 24(4):10–19

Clarke A, Liu X (1994) Interannual sea level in the northern and eastern Indian Ocean. J Phys Oceanogr 24:1224–1235

Dong DP, Zhou WD, Yang Y, Du Y (2008) Diagnostic calculations and discussions on main outflow passage of South China Sea. J Trop Oceanogr 27(6):1–5

Fang G, Chen H, Wei Z, Wang Y, Wang X, Li C (2006) Trends and interannual variability of the South China Sea surface winds, surface height, and surface temperature in the recent decade. J Geophys Res 111:C11S16. doi:10.1029/2005JC003276

Fang G, Wang Y, Wei Z, Fang Y, Qiao F, Hu X (2009) Interocean circulation and heat and freshwater budgets of the South China Sea based on a numerical model. Dyn Atmos Oceans 47:55–72

Feng M, Meyers G, Pearce A, Wijffels S (2003) Annual and Interannual Variations of the Leeuwin Current at 32°S. J Geophys Res 108(11):3355. doi:10.1029/2002JC001763

Feng M, Li Y, Meyers G (2004) Multidecadal variations of Fremantle sea level: footprint of climate variability in the tropical Pacific. Geophys Res Lett 31:L16302. doi:10.1029/2004GL019947

Hu J, Kawamura H, Hong H, Qi Y (2000) A review on the currents in the South China Sea: seasonal circulation, South China Sea Warm Current and Kuroshio intrusion. J Oceanogr 56:607–624

Johnson HL, Garrett C (2006) What fraction of a Kelvin wave incident on a narrow strait is transmitted? J Phys Oceanogr 36:945–954

Klein SA, Soden BJ, Lau NC (1999) Remote Sea surface variations during ENSO: evidence for a tropical atmospheric bridge. J Clim 12(4):917–932

Levitus S, Antonov JI, Boyer TP (2005) Warming of the world ocean, 1955–2003. Geophys Res Lett 32:L02604

Metzger EJ, Hurlburt HE (1996) Coupled dynamics of the South China Sea, the Sulu Sea and the Pacific Ocean. J Geophys Res 101(C5):12331–12352

Qu T (2000) Upper layer circulation in the South China Sea. J Phys Oceanogr 30:1450–1460

Qu T, Song YT (2009) Mindoro Strait and Sibutu Passage transports estimated from satellite data. Geophys Res Lett 36:L09601. doi:10.1029/2009GL037314

Qu T, Kim YY, Yaremchuk M, Tozuka T, Ishida A, Yamagata T (2004) Can Luzon Strait transport plays a role in conveying the impact of ENSO to the South China Sea? J Clim 17:3644–3657

Schiller A, Oke PR, Brassington G, Entel M, Fiedler R, Griffin DA, Mansbridge JV (2008) Eddy-resolving ocean circulation in the Asian–Australian region inferred from an ocean reanalysis effort. Prog Oceanogr 76(3):334–365

Spall MA, Pedlosky J (2005) Reflection and transmission of equatorial Rossby Waves. J Phys Oceanogr 35(3):363–373

Su JL (2004) Overview of the South China Sea circulation and its influence on the coastal physical oceanography outside the Pearl River Estuary. Cont Shelf Res 24:1745–1760

Tessler ZD, Gordon AL, Pratt LJ, Sprintall J (2010) Transport and dynamics of the Panay Sill overflow in the Philippine Seas. J Phys Oceanogr 40:2679–2695. doi:10.1175/2010JPO4395.1

Tian J, Yang Q, Liang X, Xie L, Hu D, Wang F Qu T (2006) Observation of Luzon Strait transport. Geophys Res Lett 33:L19607. doi:10.1029/2006GL026272

Wang C, Wang W, Wang D, Wang Q (2006a) Interannual variability of the South China Sea associated with El Niño. J Geophys Res 111:C03023. doi:10.1029/2005JC003333

Wang D, Liu Q, Huang RX, Du Y, Qu T (2006b) Interannual variability of the South China Sea throughflow inferred from wind data and an ocean data assimilation product. Geophys Res Lett 33:L14605. doi:10.1029/2006GL026316

Yaremchuk M, McCreary JL, Yu ZJ, Furue R (2009) The South China Sea throughflow retrieved from climatological data. J Phys Oceanogr 39:753–767